Indian Journal of Technology
Vol. 28, June-August 1990, pp. 413-427

Solid state electrochemical sensors in process control

K T Jacob & Tom Mathews

Department of Metallurgy, Indian Institute of Science, Bangalore 560 012, India

The basic principles of operation of gas sensors based on solid-state galvanic cells are described. The polarisation of the electrodes can be minimised by the use of point electrodes made of the solid electrolyte, the use of a reference system with chemical potential close to that of the sample system and the use of graded condensed phase reference electrodes. Factors affecting the speed of response of galvanic sensors in equilibrium and non-equilibrium gas mixtures are considered with reference to products of combustion of fossil fuels. An expression for the emf of non-isothermal glavanic sensors and the criterion for the design of temperature compensated reference electrodes for non-isothermal galvanic sensors are briefly outlined. Non-isothermal sensors are useful for the continuous monitoring of concentrations or chemical potentials in reactive systems at high temperatures. Sensors for oxygen, carbon, and alloying elements (zinc and silicon) in liquid metals and alloys are discussed. The use of auxiliary electrodes permit the detection of chemical species in the gas phase which are not mobile in the solid electrolyte. Finally, the cause of common errors in galvanic measurements and tests for correct functioning of galvanic sensors are given.

Solid state galvanic sensors for the determination of the partial pressure of a variety of species have gained popularity with the advent of robotics in chemical and metallurgical industries and increasing awareness of the consequence of environmental pollution. In industry they are used for control of fossil fuel combustion, control of exhaust gases from automobile engines and emissions from non-ferrous smelters, monitoring and control of atmospheres in metallurgical heat treatment furnaces and rapid determination of activities or concentrations of solutes in liquid metals and alloys. Devices for measuring the oxygen content in liquid melts and gases are now commercialy available. The operation of automobile engines at the stoichiometric air fuel ratio (A/F) improves engine efficiency and minimizes the emission of toxic gases like CO and NO_x. Sufficient amount of oxygen is supplied to convert all hydrocarbons to CO_2 and H_2O. The proposed lean-burn car engines require an oxygen sensor having adequate speed of response, ruggedness in the corrosive environment of the exhaust, long-term stability and low cost when produced in large amounts. Other interesting applications include the monitoring of the oxygen content of exhaled air in intensive care units and the control of the air-gas ratio in domestic condensing boilers. If excess air is reduced, the dew point of water vapour in the flue is lowered so that the recovery of latent heat by condensation is increased. Control of air-gas ratio can be achieved continuously with a permanently installed oxygen sensor. The classical (mostly infrared spectroscopic) methods of gas analyses are far from being suitable for these new types of application.

The major advantages of solid state galvanic sensors are: (a) they can be used 'in situ' in high temperature systems, (b) the emf generated can be measured with high precision, (c) since the output is an electrical potential, it can be readily used to actuate control circuits, (d) the generated emf is independent of the dimensions of the galvanic cell, which permits miniaturization and integration into microelectronic devices, (e) the emf measured is a function of the logarithm of the ratio of partial pressures; hence the sensor covers a wide range with reasonable precision, (f) the electrical signal generated is selective for the mobile species in the solid electrolyte, (g) the cell emf is a function of bulk properties and is independent of specific electrostatic potential distributions at the boundary, and (h) the solid state cell is rugged and leak proof.

This article will focus on the basic principles of operation of solid-state galvanic sensors, some critical properties of solid electrolytes and electrode systems, and their response characteristics, use of auxiliary electrodes, latest developments in non-isothermal sensors, test for correct functioning and directions for furure research.

Theory

A solid state galvanic sensor consists of an ionic or mixed conducting solid which separates the gas from a reference electrode of fixed chemical potential. Between the sample gas and reference electrode, if there exists a difference of the chemical potential of the mobile species in the solid electrolyte, there will be a particle flux in the solid along the gradient. For diffusion in an activity gradient and electric field the flux is given by[1]

$$j_i = -c_i b_i(\text{grad}\,\mu_i + z_i q\,\text{grad}\,\phi) = -c_i b_i\,\text{grad}\,\eta_i \quad \ldots(1)$$

where c, b, q, z, μ, ϕ and η are concentration, mobility, elementary charge, valency of the species, chemical potential, electrostatic potential and electrochemical potential, respectively. The subscript i refers to the component i.

Under steady state conditions when no current is drawn through the solid, charge neutrality has to be maintained at every point. This requires

$$\sum_i z_i j_i = 0 \quad \ldots(2)$$

Combining Eqs (1) and (2) gives

$$-\sum_i c_i z_i b_i\,\text{grad}\,\eta_i = 0 \quad \ldots(3)$$

The absolute mobility of the component i can be written as

$$b_i = u_i/(|z_i|q) = \sigma_i/(z_i^2 c_i q^2) \quad \ldots(4)$$

where u and σ are electrical mobility and electrical conductivity respectively. Combining Eqs (3) and (4) and solving for grad ϕ, we get

$$\text{grad}\,\phi = -q^{-1}\sum_i (t_i/z_i)\text{grad}\,\mu_i \quad \ldots(5)$$

where $\sigma_i/\Sigma\sigma_i$ is the transference number (t_i). Because of the partial pressure difference between the sample gas and the reference electrode the ions and electrons tend to diffuse along the gradient. According to Eq. (5) this tendency of ions and electrons is compensated by an electric field that opposes ionic motion. In other words, the sensor develops an emf by the separation of charged species moving under the influence of concentration gradients. The emf generated is measured as an integral quantity between the left and right-hand electronic conducting leads.

$$E = \phi^r - \phi^l = -q^{-1}\int_l^r \sum_i (t_i/z_i)\mathrm{d}\mu_i \quad \ldots(6)$$

In galvanic sensors predominantly ionic conducting solids are used. When there is only one mobile species:

$$E = \phi^r - \phi^l = -q^{-1}\int_l^r (t_i/z_i)\mathrm{d}\mu_i \quad \ldots(7)$$

The integral of Eq. (7) can be split into parts corresponding to electronic conducting leads and ionic conducting solid electrolyte. Thus we can write for a cell incorporating a pure ionic conductor ($t_{ion} > 0.99$)[2]:

$$E = q^{-1}[\mu_e^r - \mu_e'' + 1/z_i(\mu_i' - \mu_i'') + \mu_e' - \mu_e^l] \quad \ldots(8)$$

where single and double primes indicate the left and right-hand phase boundaries of the solid electrolyte. If the following equilibrium

$$X_i = X_i^{z+} + z_i e \quad \ldots(9)$$

exists at the electrode/electrolyte interface, the chemical potentials can be expressed as

$$\mu_i^* = \mu_i + z_i\mu_e \quad \ldots(10)$$

where μ_i^* and μ_i are the chemical potentials of the neutral atoms and ions respectively. Because of the very high electron concentration the chemical potential of electrons are constant in each metallic lead. Eq. (8) can therefore be written as

$$E = (z_i q)^{-1}(\mu_i^{*\prime} - \mu_i^{*\prime\prime}) \quad \ldots(11)$$

Since

$$\mu_i^* = \mu_i^{*0} + RT\ln a_i = \mu_i^0 + RT\ln(P_i/P_i^0) \quad \ldots(12)$$

where a_i represents the activity, P_i and P_i^0 represent the partial pressure of i over the electrode and pure i respectively.

$$E = (RT/z_i q)\ln(a_i^{*\prime}/a_i^{*\prime\prime}). \quad \ldots(13)$$

This is the familiar Nernst equation. In subsequent use of the equation the symbol* representing neutral species will be omitted and all activities refer only to neutral species. Deviations from the ideal Nernst behaviour are caused by the absence of a sudden transition from ionic to electronic conduction at the electrolyte/electrode boundary.

Sensors for Oxygen

The principle application of oxide solid electrolytes to date has been in galvanic sensors for measuring the partial pressure of oxygen. In research laboratories such cells have been extensively employed in the generation of accurate thermody-

namic data (free energies, enthalpies, and entropies of formation) on oxides and on solutions of oxygen in metals and alloys. In industry these cells are frequently used for measuring the partial pressure of oxygen in gaseous environments and for monitoring the activity of oxygen in molten metals and alloys. For example, in wire bar casting of copper oxygen sensors are used continuously. In steel industry oxygen sensors are used as single immersion devices that are discarded after use. Control of the oxygen content is often essential for both ingot and continuously cast steel. The key to better control of deoxidation of liquid steel is a sensing device for rapid measurement of the concentration of oxygen. In nuclear industry on-line monitoring of oxygen in liquid sodium is important for fast breeder reactor development. The other important uses are control of combustion in boilers burning fossil fuels to maximise efficiency and minimise the generation of CO[3,4], monitoring and control of atmospheres in metallurgical heat treatment furnaces[5], control of car exhaust gases for protection of three way catalyst systems[6], control of P_{O_2} in laboratory applications using pump-gauge devices[7,8] and oxygen sensors in automobile engines[9,10]. Millions of automobiles have been fitted with oxygen sensors during the last decade.

The cell

$$O_2(P'_{O_2}),\ \mathrm{Me}\left|\begin{matrix}O^{2-}\ \text{conducting}\\ \text{solid electrolyte}\end{matrix}\right|\mathrm{Me},\ O_2(P''_{O_2}) \qquad \ldots (\mathrm{I})$$

generates an emf, E, between the metal electrodes, Me,

$$E=(RT/4F)\int_{P'_{O_2}}^{P''_{O_2}} t_{ion}\,\mathrm{d}(\ln P_{O_2}) \qquad \ldots (14)$$

where R is the gas constant, T the absolute temperature, F the Faraday constant and t_{ion} the transport number of the mobile ion (oxygen). If t_{ion} is close to unity then Eq. (14) simplifies to

$$E=(RT/4F)\ln P''_{O_2}/P'_{O_2} \qquad \ldots (15)$$

The metal electrodes may be Pt, Ag or any other material that catalyses the oxygen exchange reaction between the gas and the solid electrolyte.

Solid electrolytes exhibit predominant ionic conductivity (ionic transferance number, $t_{ion}>0.99$) only over a limited range of temperature and chemical potential. So electrolytic conduction domain is an important factor limiting the application of solid electrolytes in galvanic sensors. A schematic representation of the conduction

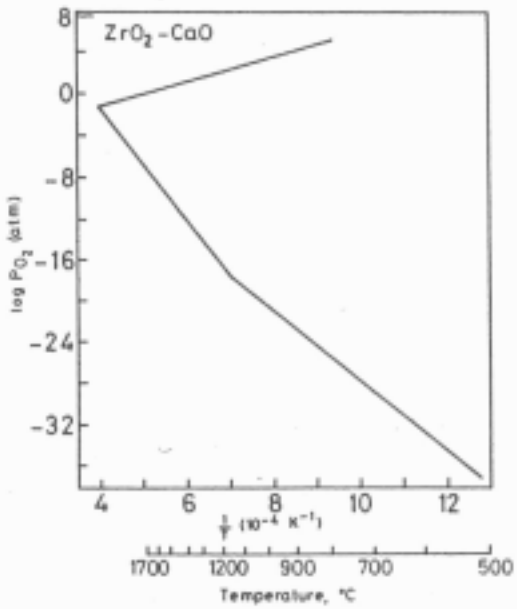

Fig. 1—Electrolytic conduction domain ($t_{ion}>0.99$) of ZrO_2 (15 mole % CaO)

domain of calcia stabilised zirconia is shown in Fig. 1. At low oxygen partial pressures, the partial electronic conductivity increases because of electron generation

$$O_O^x = 1/2O_2 + V_O^{\cdot\cdot} + 2e$$

and at high oxygen partial pressures a similar effect takes place as a result of hole generation

$$V_O^{\cdot\cdot} + 1/2\,O_2 = O_O^x + 2h$$

Thus at low and high oxygen partial pressures t_{ion} will be less than unity. The oxygen partial pressure range over which ionic conductivity predominates reduces with increasing temperature. Even within the ionic conduction domain, electron and hole conductivities have finite values. The residual electron or hole conductivity gives rise to electrochemical permeability or semipermeability of the migrating species in the solid electrolyte.

Galvanic oxygen sensors incorporate oxygen ion conductors like ZrO_2, CeO_2 or ThO_2 as solid electrolytes. Ionic conductivity of these oxides is enhanced by doping with aliovalent oxides which generate high concentration of anionic vacancies. Electrolytes based on ZrO_2 (ZrO_2-Y_2O_3, ZrO_2-CaO or ZrO_2-MgO) are most commonly used at the present time. Ionic conductivity increases with the type of dopant and its concentration in the order $Yb_2O_3 > Y_2O_3 > CaO > MgO$[11]. These dopants stabilise the cubic structure of zirconia at lower temperatures. Lower dopant levels achieve

partial stabilization, resulting in a cubic phase with tetragonal precipitates. Fully stabilized zirconia has lower thermal shock resistance than partially stabilized material. Recent work has shown that suitably prepared partially stabilised zirconia can have conductivities adequate for sensors, with high fracture toughness providing a distinct advantage[12]. A requirement for accurate measurement is that electronic partial conductivity should be very small so that t_{ion} in Eq. (14) is close to unity. Further, the physical permeability should be negligible and thermal shock resistance should be sufficient to prevent cracking during thermal cycling.

The electrode reaction can be represented as,

$$1/2O_2 + 2e + V_O^{\cdot\cdot} = O_O^x \quad \ldots (16)$$

where $V_O^{\cdot\cdot}$ and O_O^x are oxygen vacancies and oxygen ions in the lattice respectively. This reaction takes place at the three-phase boundary[13-15] between the gas phase, the electrode and the electrolyte. Therefore, close contact between the electrode and electrolyte and a long three-phase boundary are essential for good results. Platinum paints which are dried first and then fired in air to burn off the organic binders provide good contact and can be a suitable electrode[16]. But at high firing temperatures recrystallization and sintering of platinum take place, reducing porosity and length of the three-phase boundary. This also happens more slowly at operating temperatures[17]. Hence the firing and operating temperatures should be minimized to maintain the activity of the electrodes[18]. Platinum electrodes can also be applied by techniques other than painting (e.g. sputtering, evaporation). Platinum electrodes behave catalytically and at elevated temperature bring the concentration of components of the gas phase at the gas-solid interface to their thermodynamic equilibrium value. The measured emf then corresponds to equilibrium P_{O_2} rather than actual. It has been found that platinum can be poisoned with lead so that the measured P_{O_2} correspond to the non-equilibrium value at temperatures above 773 K; at lower temperatures even lead poisoned platinum electrodes are catalytic[19].

Electrode Polarisation

One important factor which results in incorrect values for the concentration of oxygen in a galvanic sensor is electrode polarisation. Polarisation occurs as a result of the physical or electrochemical permeability of the solid electrolyte. While physical permeability can be reduced by using a dense form of the solid electrolyte free from interconnecting porosity, electrochemical permeability results from the intrinsic properties of the material. Because of the small but finite electronic conduction present in the solid electrolyte, a charge compensated ionic flux occurs, resulting in a mass transport of the active species across the electrolyte from an electrode of higher chemical potential to the one having a lower chemical potential of the mobile species. This phenomenon known as the electrochemical permeability or semipermeability will cause electrode polarisation, especially when the electrodes have a low thermodynamic capacity for the conducting species[20] and a large gradient of chemical potential exists across the solid electrolyte.

When gas electrodes are used, the presence of polarisation manifests as flow rate dependence of emf. Although polarisation can be reduced by increasing the flow rate, a practical limit is set by the cooling effect of the streaming gas. Asymmetric gas flows at the two electrodes can result in differential cooling and non-isothermal contributions to cell emf which are difficult to correct. A design solution to the polarisation problem is the use of a point electrode[21] shown in Fig. 2. The platinum electrode actually measures the equilibrium chemical potential of oxygen in a microsystem formed at the triple phase region among the electrode, electrolyte and gas. The oxygen flux through the electrolyte due to the semipermeability may alter the equilibrium oxygen chemical potential in the microsystem[21]. Since the ionic flux takes the lowest resistance path, this flux is dissipated at the tip of the point electrode made using the same material as the electrolyte. The measured

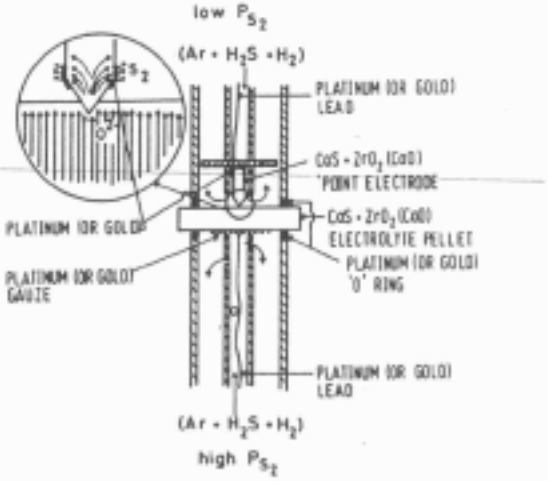

Fig. 2—A schematic representation of the CaS + (CaO)ZrO_2 point electrode for deflecting the semipermeability flux from the measuring metal electrode—a modified version[22] of the system introduced by Fouletier *et al.*[21]

composition at the platinum lead corresponds to that of the bulk gas. Jacob *et al.*[22] have shown that the performance of the point electrode can be improved by applying a porous coating of a catalyst such as Pt at the tip of the point electrode made from the solid electrolyte material. Another method of minimizing semipermeability and its effect on emf is by choosing a reference system with a chemical potential close to that of the sample system. Air is the commonly used reference gas as it is easily available and has constant compositon. For accurate measurements air should be dried and correction for barometric changes applied. Mixtures of inert gas and oxygen are not suitable for $P_{O_2} < 10^2$ Pa because of the low thermodynamic capacity of the mixture for oxygen[20]. Mixtures of $CO + CO_2$ and $H_2 + H_2O$ provide good buffered systems with low equilibrium oxygen partial pressure when the gas ratio ranges from 10^{-3} to 10^3. The usefulness of $H_2 + H_2O$ mixtures is limited by severe thermal segregation in the gas phase and the elaborate procedures required to minimize it.

Flowing gas is inconvenient for sensors that must operate inside high temperature reactors. This problem can be solved by using sealed condensed phase mixtures inert to the solid electrolyte. A two phase metal/metal oxide which generates a P_{O_2} fixed by the temperature of operation can be used. Selection of an appropriate redox system may be made from thermodynamic data on component phases or Ellingham diagram for oxides. A very wide range of P_{O_2} values can be generated using an appropriate redox system. Mixtures like $Ni + NiO$ and $Cr + Cr_2O_3$ are easily polarisable, especially when the oxygen content of the sample is higher than that established by these mixtures. In such cases an excess of the component that is being consumed due to the flux of oxygen is taken to minimize polarisation. The use of graded composition electrodes to minimize polarisation without significantly affecting the buffer capacity of the reference system has been successfully used by the authors.

Response Time

The response time for an electrochemical sensor is defined as the time taken for the sensor to achieve a specified per cent of its maximum open circuit voltage after a step change in the bulk oxygen partial pressure. For a sensor consisting of a pure electrolyte and perfectly reversible electrodes, the emf developed after a step change is constant and has the value corresponding to the Nernst equation right from the start. Since $t_{O^{2-}}$ of the equation:

$$E = (1/4F) \int_{\mu_{O_2}}^{\mu''_{O_2}} t_{O^{2-}} \, d\mu_{O_2} \qquad \ldots (17)$$

in this case is unity and can be taken out of the integral, E becomes independent of the μ-distribution and is determined by the boundary values only.

The presence of a mixed or electronic conducting phase with lower oxygen ion transport number gives rise to a slow response[23,24]. Consider a system in equilibrium with equal partial pressure of the active species at both sides of the solid electrolyte. When there is a step change in the concentration of the active species at one of the electrodes, a finite amount of the active species is taken (or released) by the electrolyte/electrode system. In practical systems the composition of the solid electrolyte depends on the partial pressure of the active species in the gas phase. Thus compositional changes are induced in the solid electrolyte because of the changes in the gas concentration. These compositional changes give rise to small deviations from the exact stoichiometry. The process of reestablishment of a new equilibrium concentration gradient in the solid electrolyte takes some time. During this transition period the emf developed may have a value different from that in the final equilibrium state. If the electrode kinetics is sufficiently rapid compared to the rate of uptake or release of active species by the solid electrolyte, deviation from the equilibrium value will not be observed. When the electrode kinetics is slow, the flux of the active species due to stoichiometric readjustment can affect the partial pressure in the microsystem around the electrodes and thus influence the emf. The redistribution of concentration of the active species is illustrated schematically in Fig. 3. Heyne and den Engelsen[24] have proposed a numerical method for the calculation of the new concentration distribution of the active species at time t after a step change in the active species concentration. They also computed new local transport numbers from the concentration distribution. For an oxide solid electrolyte with dispersed (second phase) impurity, shown schematically in Fig. 4, the emf can be represented as

$$E = (1/2nF) \Sigma t_j (\mu_{O_2}^{j\,II} - \mu_{O_2}^{j\,I})$$

where t_j is the oxygen transport number in the region j and $(\mu_{O_2}^{j\,II} - \mu_{O_2}^{j\,I})$ is the potential drop over this region. Regions with $t_{O^{2-}} = 1$ and $(\mu_{O_2}^{j\,II} - \mu_{O_2}^{j\,I})$

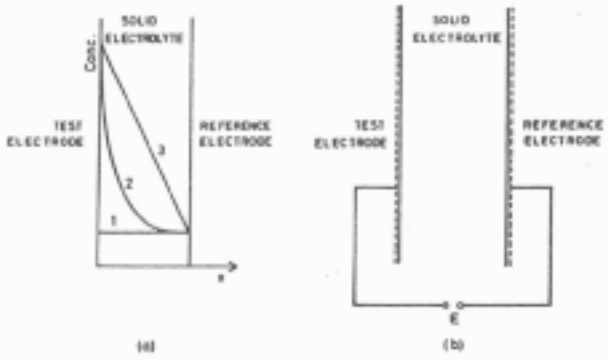

Fig. 3—Solid state electrochemical gas sensor. (a) Concentration profile in solid electrolyte after a step increase in the partial pressure of the test gas. Curve 1 shows the initial distribution; curve 2 represents an intermediate distribution and curve 3 depicts final steady state distribution. (b) Schematic representation of an electrochemical gas sensor.

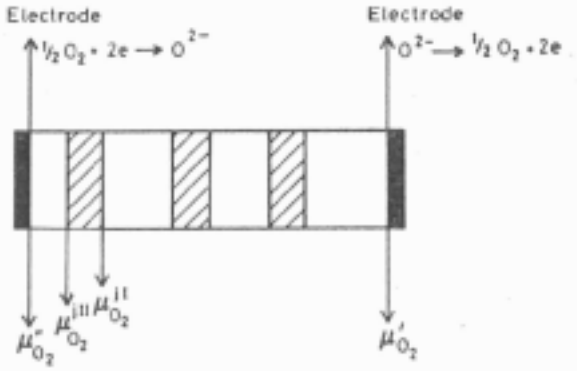

Fig. 4—A schematic diagram of an oxygen sensor based on an oxygen ion conducting solid electrolyte with second phase regions exhibiting mixed conductivity

$\neq 0$ will generate Nernstian emf. Regions with $(\mu^{III}_{O_2} - \mu^{II}_{O_2}) = 0$ do not contribute to the emf. The contributions of regions with $(\mu^{III}_{O_2} - \mu^{II}_{O_2}) \neq 0$ and $t_{O^{2-}} < 1$ will be less than the ideal value. If the solid electrolyte has a mixed conducting dispersed phase, the emf can drift for a long time when the chemical potential is altered at an electrode. The diffusion processes in the solid electrolyte are many orders of magnitude slower than the equilibratory reaction at the electrode/electrolyte interface. The composition profile will be established only after a long time. During this process the chemical potential gradient across the dispersed phase changes with time, giving rise to a varying emf contribution till the steady state profile is established. This drift in emf is only a few per cent of the emf change after the alteration[24].

In general, response time depends on a number of factors[25]:

(a) At the electrode/electrolyte interface there is a separation of charge; the charge in the electrolyte is balanced by an equal and opposite charge in the electrode. This double layer acts as a capacitor requiring the transfer of charge when the sensor emf responds to a step change in oxygen pressure.

(b) The double layer region must come to chemical equilibrium with the gas phase before the electrode potential is stabilized.

(c) Stoichiometric changes in the electrolyte introduce overvoltage due to charge transfer which perturbs the measured emf. An oxygen partial pressure gradient may be set up in the gas phase adjacent to the electrode/electrolyte interface if the flux due to the change of stoichiometry of the solid electrolyte is large. This gives rise to diffusion overvoltage. The electrode response is slowed down because of the above two overvoltages.

(d) The response of a sensor is enhanced by using electrodes having lower resistance to charge transfer.

(e) Before the electrode can respond to a P_{O_2} change that change must be transmitted to the electrode/electrolyte interface. The rate at which an oxygen pressure change reaches the electrode surface is influenced by the hydrodynamics in the gas phase.

Fouletier *et al*[26] carried out response measurements on oxygen sensors and found the sensor voltage as a function of time (t) after a step change in P_{O_2}, to follow the relation

$$E(t) - E(0) = [E(\infty) - E(0)]\exp(-t/\tau)^{1/2} \quad \ldots (18)$$

where $E(t)$, $E(0)$ and $E(\infty)$ are sensor voltages at $t = t$, $t = 0$ and $t = \infty$, respectively; τ is a characteristic time parameter, which follows an Arrhenius-type expression[26]

$$\tau = A(P_m)^{-1/2} \exp(Q_{act}/RT) \quad \ldots (19)$$

where A is a constant and P_m is the mean oxygen partial pressure, $P_m = (P_{initial} + P_{final})/2$. Combining Eq. (18) and (19), we get:

$$t = A(P_m)^{-1/2} \exp(Q_{act}/RT) \left[\ln \frac{E(\infty) - E(t)}{E(\infty) - E(0)}\right]^2 \quad \ldots (20)$$

In their experiments they found both platinum and silver electrodes responded according to Eq. (20). The response of silver electrodes was faster than that of platinum electrodes.

Based on experiments on oxygen sensors based on ZrO_2 (CaO) Anderson and Graves[27] found the diffusive mass transfer from the bulk gas to the reaction sites at the electrode/electrolyte interface to be the rate determining step. For a step change

in the oxygen partial pressure of the test gas the cell response is found to be faster for low to high partial pressure change than for the reverse. They used normalized functions, $\phi_v(t)$ and $\phi_c(t)$, given as

$$\phi_v(t) = |E(t) - E(\infty)|/|E(0) - E(\infty)| \quad \ldots (21)$$

$$\phi_c(t) = |P_{O_2}(t) - P_{O_2}(\infty)|/|P_{O_2}(0) - P_{O_2}(\infty)| \quad \ldots (22)$$

and found $\phi_c(t)$ values to be independent of the direction of the oxygen partial pressure change. The similarity in $\phi_c(t)$ values indicate the diffusive mass transfer from the bulk gas to the electrode/electrolyte interface as the rate determining step. In order to minimize the gas phase diffusion limitations, Winnubst *et al*.[28] used thin porous electrodes and increased the flow rate of the gas impinging on the electrode. They found the same kind of asymmetry as in reference 27 on going from low to high and high to low oxygen partial pressures. In their experiments oxygen partial pressure change from low to high values gave slightly different $\phi_v(t)$ and $\phi_c(t)$ values in comparison with a partial pressure change in the reverse direction. They concluded that the difference in the $\phi_c(t)$ values at a fixed temperature suggests that other processes at the gas-electrode-electrolyte interface play a role in the response behaviour. The responses of Ag[26] and Au[28] electrodes were found to be faster than the response of Pt electrodes.

In practical situations non-equilibrium gases are often encountered. Analysis of a three-component system containing gaseous oxygen, carbon dioxide and carbon monoxide that follow the reaction

$$O_2 + 2CO = 2CO_2 \quad \ldots (23)$$

has been done by Anderson and Graves[29]. Their analysis has been generalised by Maskell[25], who considered a three-component system containing gases X, Y and Z that interact according to the reaction

$$aX + bY = cZ \quad \ldots (24)$$

Three regions on each side of the electrolyte, (a) a bulk gas, (b) a gaseous boundary layer, and (c) electrode catalyst surface, are considered. The species reach the electrode surface by diffusion. The gases X, Y and Z may be monoatomic or polyatomic and can be written as X_x, Y_y and Z_z, where x, y and z represents the number of atoms of X, Y and Z in each molecule. The following three equations can be written to describe the *surface reactions:*

$$\frac{d\Gamma_X}{dt} = -xK_2\Gamma_X^x + xK_X P_X \Gamma_V^x - aK_1\Gamma_X^a\Gamma_Y^b + aK_R\Gamma_Z^c\Gamma_V^{(a+b-c)} \quad \ldots (25)$$

$$\frac{d\Gamma_Y}{dt} = -yK_4\Gamma_Y^y + yK_Y P_Y \Gamma_V^y - bK_F\Gamma_Y^b\Gamma_X^a + bK_R\Gamma_Z^c\Gamma_V^{(a+b-c)} \quad \ldots (26)$$

$$\frac{d\Gamma_Z}{dt} = -zK_6\Gamma_Z^z + zK_Z P_Z \Gamma_V^z + cK_F\Gamma_X^a\Gamma_Y^b - cK_R\Gamma_Z^c\Gamma_V^{(a+b-c)} \quad \ldots (27)$$

where Γ_i is the fractional surface coverage of the species i, and Γ_V is the fractional surface coverage by vacancies. P_X, P_Y and P_Z are the partial pressures of X, Y and Z adjacent to the electrode surface. K_X, K_Y and K_Z are the adsorption rate constants for the subscript species and K_2, K_4 and K_6 are the desorption rate constants; K_R and K_F are the reverse and forward rate constants for the surface reaction. The above three equations state that the rate of change in the fractional coverage of the species is a function of adsorption, desorption, forward and reverse reaction rates. These equations are based on isothermal Langmuir-type kinetics[30].

The rate of transport of species from the bulk gas across the boundary layer to the electrode surface can be described by the following expressions.

$$\frac{dP_X}{dt} = -K_1(P_X - P'_X) - K_X P_X \Gamma_V^x + K_2\Gamma_X^x \quad \ldots (28)$$

$$\frac{dP_Y}{dt} = -K_3(P_Y - P'_Y) - K_Y P_Y \Gamma_V^y + K_4\Gamma_Y^y \quad \ldots (29)$$

$$\frac{dP_Z}{dt} = -K_5(P_Z - P'_Z) - K_Z P_Z \Gamma_V^z + K_6\Gamma_Z^z \quad \ldots (30)$$

where P'_X, P'_Y and P'_Z refer to the partial pressures of the species X, Y and Z in the bulk; K_1, K_3 and K_5 describe the mass transfer coefficients between the bulk gas and the boundary layer.

The surface concentrations are determined by adsorption, desorption and chemical reaction between unionised species. In this model only reactions between adsorbed molecules or atoms is considered whereas reaction between adsorbed and gaseous species is also possible. Further, only chemical reaction between X and Y is considered and electrochemical redox reactions are ignored.

In spite of these simplifications the analysis gives an insight into the electrode/electrolyte interface process. Two potential determining reactions are considered

$$X + V_X^{n'} + ne \underset{K_8}{\overset{K_7}{\rightleftharpoons}} X_X^x + \Theta \qquad \ldots (31)$$

$$(c/a)Z + V_X^{n'} + ne \underset{K_{10}}{\overset{K_9}{\rightleftharpoons}} X_X^x + (b/a)Y \qquad \ldots (32)$$

where $V_X^{n'}$, X_X^x and Θ are charged anion vacancy, anions in the lattice and a vacant surface site on the electrolyte respectively. Under steady state conditions the anodic current of one reaction is equal in magnitude to the cathodic current of the other so that the resultant current is zero. Then the reaction rate theory gives

$$(K_7\Gamma_X + K_9\Gamma_Z)w\exp(-nF\phi/2RT) = (K_8\Gamma_V + K_{10}\Gamma_Y)X_s\exp(nF\phi/2RT) \qquad \ldots (33)$$

where w and X_s are the surface concentration of $V_X^{n'}$ and X_X^x respectively.

$$\frac{nF\phi}{RT} = \ln\frac{K_7}{K_8}\left\{\frac{(\Gamma_X/\Gamma_V) + (K_9/K_7)(\Gamma_Z^{(c/a)}/\Gamma_V)}{1 + (K_{10}/K_8)(\Gamma_Y^{(b/a)}/\Gamma_V)}\right\}\frac{w}{X_s} \qquad \ldots (34)$$

A similar analysis at the reference electrode will give

$$nF\phi'/RT = \ln[(K_7/K_8)(\Gamma_X/\Gamma_V)'(w/X_s)] \qquad \ldots (35)$$

Assuming that (w/X_s) is uniform across the electrolyte, we get the sensor emf as

$$E = \phi - \phi' = \frac{RT}{nF}\ln\left\{\frac{(\Gamma_X/\Gamma_V) + (K_9/K_7)(\Gamma_Z^{(c/a)}/\Gamma_V)}{1 + (K_{10}/K_8)(\Gamma_Y^{(b/a)}/\Gamma_V)}\right\} \times \left(\frac{\Gamma_V}{\Gamma_X}\right) \qquad \ldots (36)$$

Anderson and Graves[29] have solved Eqs (25)-(36) using a numerical technique, considering the reaction (23) to be the most important in determining the emf of oxygen sensors when exposed to reactive gases coming from internal combustion engines. Their analysis indicates that with non-equilibrium bulk gas mixtures the cell emf corresponds to equilibrium oxygen partial pressures, when (a) mass transfer between bulk gas and surface boundary layers is slow relative to the rate of surface reactions and (b) the reactants have identical mass transfer coefficients.

The response of the sensor to the reactive gases is dependent upon the choice of the electrode material. In many applications, such as combustion control, where the equilibrium partial pressure of oxygen is to be measured, Pt is preferred because of its high catalytic activity. However, in situations where the actual oxygen content of a reactive gas mixture is required non-catalytic electrodes are preferred. Halland[31] has found that silver deposited on platinum is non-catalytic while gold is slightly catalytic.

Effect of Temperature on emf

The variation of the emf with sensor temperature is expressed by

$$dE/dT = (-R/nF)\ln(P_1/P_2) \qquad \ldots (37)$$

In an oxygen sensor using air as reference, temperature coefficients of approximately 0.5 and 1.0 mV K^{-1} are anticipated at 10^{-5} and 10^{-15} atmospheres of partial pressure of oxygen in the sample gas (inert gas + oxygen mixture).

In a cell using condensed phase mixtures as the reference electrode, the reference oxygen potential is fixed by the dissociation of the oxide;

$$M_mO_{2n} = mM + nO_2 \qquad \ldots (38)$$

For a cell,

$$M, M_mO_{2n}, O_2(P'_{O_2}), Pt|SE|Pt, O_2(P''_{O_2}) \qquad \ldots (II)$$

The temperature differential can be expressed as

$$dE/dT = -1/(2F)[(m/n)S^\circ_M - (1/n)S^\circ_{M_mO_{2n}} + S^\circ_{O_2} - R\ln P''_{O_2}] \qquad \ldots (39)$$

$$dE/dT = -1/(2F)[\Delta S^\circ_r - R\ln P''_{O_2}] \qquad \ldots (40)$$

where ΔS°_r is the standard entropy change for the reaction (38). The relative magnitude of the terms in the bracket can be obtained from the thermochemical tables[32]. The value of ΔS°_r is large (~ 175 J $K^{-1}mol^{-1}$) and corresponds to -0.4 mV K^{-1}. The terms $(m/n)\ S^\circ_M$ and $-(1/n)\ S^\circ_{M_mO_{2n}}$ are of similar magnitude and they tend to cancel. The final term $R\ln P''_{O_2}$ is the same as that found in sensors with gaseous reference electrodes. Hence the temperature coefficient of oxygen sensors with condensed phase mixtures as reference is always higher by ~ 0.4 mV K^{-1}. Hence the sensors using condensed phase mixtures as reference electrodes require more precise temperature control than those with gaseous reference.

Oxygen Probes for Liquid Metals and Alloys

In steel making process low oxygen contents are often essential for both ingot and continuously cast steel. The key to better control of deoxidation of liquid steel is a sensing device which rapidly measures the concentration of oxygen. Usually the oxygen probe consists of a tube or pellet of zirconia. Reference electrodes may be Pt-air, Mo-MoO_2 or Cr-Cr_2O_3. The electrical contact to molten steel is made with a rod or tube of steel or molybdenum. The oxygen potentials encountered in steel are sometimes below the electrolytic conduction boundary ($t_{ion} > 0.99$) for zirconia electrolytes. According to Schmalzried's analysis[33], the emf for oxide electrolytes with a mixed ionic and electronic conduction at low oxygen partial pressures is

$$E = (RT/F)\ln\{P_e^{1/4} + P_{O_2}^{1/4}(\text{ref})\}/\{P_e^{1/4} + P_{O_2}^{1/4}\} \quad \ldots (41)$$

where the parameter P_e is defined as the oxygen partial pressure at which ionic and electronic conductivities are equal. Using the experimentally determined value for the parameter P_e, the relation between E and chemical potential or activity of oxygen in steel can be derived. Consider the reaction,

$$1/2\ O_2 = [O]_{Fe}$$

where the standard state for dissolved oxygen is taken as an infinitly dilute solution in iron in which activity is equal to wt%. The partial pressure of oxygen over liquid iron is given by

$$P_{O_2}(\text{Fe}) = (a_O/K_O)^2 = (\%\ O.f_O)^2$$

where K_O is the equilibrium constant for oxygen dissolution in liquid iron. The activity of oxygen can therefore be expressed as

$$a_O = \exp(-\Delta G_O^\circ/RT)\{[P_e^{1/4} + P_{O_2}^{1/4}(\text{ref})] \times \exp(-EF/RT) - P_e^{1/4}\}^2 \quad \ldots (42)$$

where ΔG_O° is the standard free energy change for the dissolution of oxygen in iron.

Romero *et al.*[34] have measured low oxygen activities in Fe-O-C melts at varying carbon contents. Measurements were done in Fe-O-C melts up to 4 wt% C under pure CO gas. At controlled P_{CO}, oxygen activity in molten Fe-C alloys is closely related to carbon activity. Based on Eq. (42) for the cell

$$\text{Fe-O-C}|\text{ThO}_2(\text{Y}_2\text{O}_3)||\text{Cr}, \text{Cr}_2\text{O}_3 \quad \ldots (\text{III})$$

and the free energy for the reaction

$$[C]_{Fe} + [O]_{Fe} = CO(g) \quad \ldots (43)$$

where standard states for C and O are infinitly dilute sqlutions in liquid iron where activity is equal to wt%,

$$\Delta G_{43}^\circ = RT \ln P_{CO}/a_O \cdot a_C \quad \ldots (44)$$

one can construct a nomograph correlating the cell emf with oxygen activity and carbon content in the liquid iron at temperatures ranging from 1573 K to 1973 K and $P_{CO} = 10^5$Pa (ref. 35). Oxygen activity may be expressed as

$$\log a_O = -\log \text{wt\%[C]} - e_C^C \cdot \text{wt\%[C]} - \Gamma_C^C \cdot \text{wt\%[C]}^2 - \log K_{43} \quad \ldots (45)$$

The oxygen potential of a steel melt can be related to the carbon potential when the partial pressure of CO is well defined. Thus sensors for monitoring carbon can be designed based on oxide solid electrolytes provided a fixed partial pressure of CO is maintained over the melt through a capillary connection.

Iwase and Mori[35] have developed an analytical instrument for the determination of carbon in iron and steel using a solid state cell. A metal sample containing carbon placed in a SiC resistance furance was combusted at ~1700 K in a stream of pure oxygen. The partial pressure of oxygen in the gas phase was measured as a function of time down stream from the furnace with the cell.

$$\text{air, Pt}|\text{ZrO}_2(\text{CaO})|\text{O}_2(\text{CO}_2), \text{Pt} \quad \ldots (\text{IV})$$

The carbon content of the sample was determined from the change in the emf of the cell.

$$\text{wt\% C} = (4800\eta_{O_2}F/RTW)\int \Delta E\, dt \quad \ldots (46)$$

where η_{O_2} is the flow rate of pure oxygen at the inlet of the SiC furnace and t is the time.

Sensors for Zinc in Copper

At the casting temperature of molten brass, it is very difficult to control the zinc concentration because of its high affinity for oxygen to form ZnO and its high vapour pressure. The oxygen concentration of molten brass at saturation with ZnO is of the order of a few ppm. Hence in commercial practice brass is always saturated with ZnO. Therefore, oxygen potential determination in brass with a solid state sensor can be used to calculate Zn activity and thereby zinc content in molten brass.

Wilder and Galin[36] have shown that the cell

$$\text{Pt}|\text{Ni} + \text{NiO}||\text{CSZ}||\text{Zn (in molten brass)} + \text{ZnO}|\text{Ta} \quad \ldots (\text{V})$$

can be used to determine the Zn content of Cu-Zn alloys at 1268 K. The cell emf after correction for the junction between Pt and Ta is

$$E = -1/2F\{\Delta G^\circ_f(ZnO) - \Delta G^\circ_f(NiO) - RT\ln a_{Zn}\} \quad \ldots (47)$$

where $\Delta G^\circ_f(ZnO)$ and $\Delta G^\circ_f(NiO)$ are the standard molar free energies of formation of the oxides and a_{Zn} is the activity of Zn in molten brass.

Cells of this type may also be used to determine the nickel content in cupro-nickels, chromium in stainless steels and other alloy systems which are expected to be saturated with respect to a stable oxide in normal processing operations.

Sensors for Hydrogen

Hydrogen is used in a variety of industrial situations such as synthesis of ammonia, methanol and other chemicals, petroleum refining, chemical reduction of oxides and as a fuel. Many solid metals like Zr and Ti readily absorb hydrogen leading to the precipitation of brittle hydrides. Hydrogen evolved during the corrosion of metals may cause damage by embrittling the corroding metal leading to blisters in mild steel and catastrophic failure in high alloy steels. The detection and monitoring of hydrogen in ambient atmosphere and as a dissolved species in metals is essential for safe handling of hydrogen fuel and for controlling environmental degradation of materials.

Solid state electrochemical room-temperature hydrogen sensors have been developed[37-39]. There are a variety of proton conducting electrolytes, like hydrogen uranyl phosphate tetrahydrate (HUP), potassium dihydrogen orthophosphate, and zirconium oxide hydroxide for use in the temperature range 282-323 K. At elevated temperatures anhydrous potassium hydroxide and hydronium substituted β-alumina may be used. Out of these HUP has the highest protonic conductivity in the range 282-323 K and excellent formability.

Sensors for hydrogen using HUP have been reported[37-39] based on the Nernst equation. The cell configuration is

(Water vapour) $H'_2 + Ar'$ |Pd or Pt + HUP||HUP||Pd or Pt + HUP| (Water vapour) $H''_2 + Ar''$ ... (VI)

One of the major problems associated with the development of a hydrogen sensor is the fabrication of stable and reversible solid reference electrodes. Gaseous hydrogen as reference electrode is of limited interest in practical applications. Schoonman *et al.*[38] used a mixture of Pd and PdH_2 as a reference electrode, but PdH_2 was found to decompose gradually. Hydrogen tungsten bronze (H_xWO_3) reference electrode has been developed by Lyon and Fray[39] and the sensor is found to exhibit Nernstian response. The cell can be represented as

$WO_3 + H_xWO_3$|HUP|Pd, H_2 ... (VII)

The electrode reactions can be written as

$$x/2H_2 = xH^+ + xe \quad \ldots (48)$$

$$xH^+(HUP) + xe + WO_3 = H_xWO_3 \quad \ldots (49)$$

It has been found recently that the hydrogen tungsten bronze reference potential varies slightly for each probe and also changes with time. Such variations are found to be random and hence the sensor requires repeated calibration. The composite electrodes, γ-MnO_2/HUP/acetylene black and (α and β) PbO_2/HUP/acetylene black have been found to be reversible to hydrogen insertion into the lattice of the oxides[40]. Hydrogen sensors are developed using these reference electrodes. The cell can be represented as[41]

Metal|test gas, Pt black||HUP||γ-MnO_2|HUP|acetylene black ... (VIII)

Use of Auxiliary Electrodes

Sensors for gaseous species

Sensors with auxiliary electrodes can be used to detect those gaseous species which do not have a high mobility in a solid electrolyte. Auxiliary electrodes convert the activity of the species to be detected into an equivalent chemical potential of the mobile species in the solid electrolyte.

Auxiliary phases should be idealy dispersed in the electrolyte to give intimate contact between phases. This helps in fast equilibration. Other methods like sputtering and electrochemical deposition of auxiliary phases as thin layers on to the electrolytes are also employed. When an impervious coating of auxiliary electrode which is not a predominantly ionic conductor is applied, the thickness should be minimized to keep the chemical potential gradient across the coating to a negligible value.

Gas sensors with auxiliary electrodes for S_2, SO_x and CO_x

Sensors for sulphur[42-45], SO_x ($x = 2,3$)[46-48] and CO_x ($x = 1, 2$)[49] have been developed. Solid electrolytes CaF_2, β-alumina, Nasicon and CSZ have

been used in sensors to measure sulphur potential with sulphide auxiliary electrodes[42-45]. The cells can be represented as

$$Pt, S'_2, CaS|CaF_2|CaS, S''_2, Pt \quad \ldots (IX)$$

$$Pt, S'_2, Na_2S|\beta\text{-alumina}|Na_2S, S''_2, Pt \quad \ldots (X)$$

$$Pt, S'_2|CaS + (CaO)ZrO_2|S''_2, Pt \quad \ldots (XI)$$

Sensors for SO_x using electrolytes CaF_2, β-alumina or Nasicon were developed by Jacob and coworkers[46-48]. The cells may be represented as

$$Pt|O'_2 + SO'_2 + SO'_3|CaF_2 + CaSO_4||CaF_2|| \\ CaF_2 + CaSO_4|SO''_3 + SO''_2 + O''_2|Pt \quad \ldots (XII)$$

$$Pt|O'_2 + SO'_2 + SO'_3|Na_2SO_4||\beta\text{-alumina or Nasicon} \\ Na_2SO_4|SO''_3 + SO''_2 + O''_2|Pt \quad \ldots (XIII)$$

A schematic diagram of an SO_x sensor based on β-alumina solid electrolyte is shown in Fig. 4. The sensors based on CaF_2 solid electrolyte have been found to give a sluggish response, whereas those based on β-alumina and Nasicon give rapid response. The response curves of the sensor based on β-alumina solid electrolyte are shown in Fig. 5. The cell

$$Au, CO_2 + O_2|Na_2CO_3||Na^+ \text{ ion conductor}||O_2, Au \quad \ldots (XIV)$$

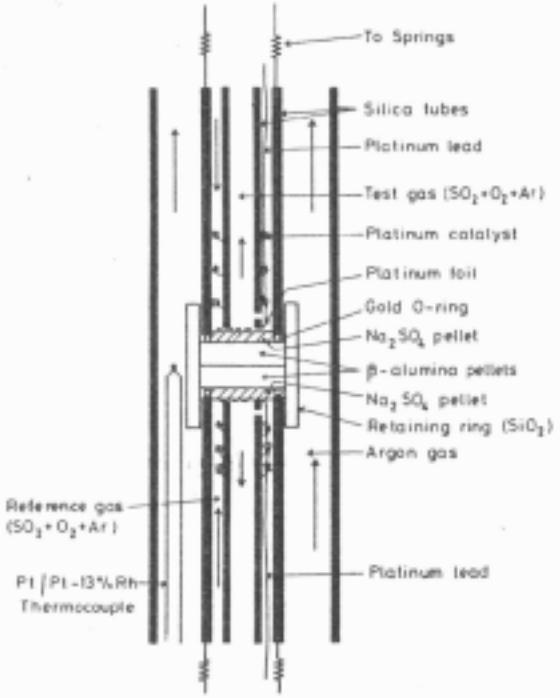

Fig. 5—Schematic representation of an SO_x sensor based on β-alumina[47]

with Na_2CO_3 as the auxiliary electrode has been designed by Maruyama *et al.*[49] for sensing CO_2.

One of the major advantages of the use of auxiliary electrodes is the large variety of solid electrolytes that may be used for a given application. The use of auxiliary electrodes expands the list of species that can be detected by any given solid electrolyte.

Sensors for alloying elements using auxiliary electrodes

Silicon in hot metal—Hot metal produced by the iron blast furnace contains appreciable amounts of silicon ranging from about 0.3 to 1.5 wt%. The production of low silicon hot metal results in appreciable cost savings in integrated steel plants. A sensor for silicon in hot metal will be a valuable aid to external desiliconisation.

Since no solid electrolyte is known at the present time in which silicon is the mobile species, a zirconia-based solid electrolyte may be used with an auxiliary electrode that will convert the activity of silicon into an equivalent chemical potential of oxygen. An electrochemical technique has been developed by Iwase[50] for in situ determination of the concentrations or activity of silicon in hot metal incorporating magnesia-stabilised zirconia as the solid electrolyte and a mixture of $ZrO_2 + ZrSiO_4$ as the auxiliary electrode. The electrochemical cell can be represented as

$$Mo|Mo + MoO_2||ZrO_2(MgO)||ZrO_2 + ZrSiO_4| \\ Si\,(in\ Fe)||Fe \quad \ldots (XV)$$

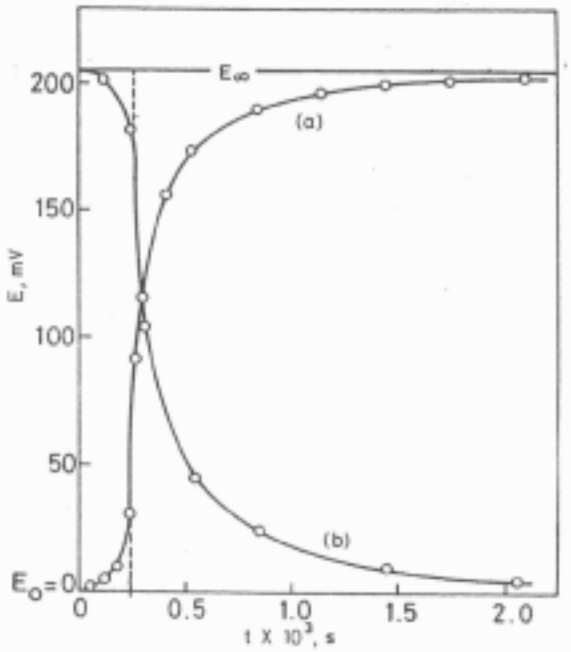

Fig. 6—Variation of open-circuit voltage with time following a step change in gas composition at 750 K [(a) Pressure increase; (b) pressure decrease[47]]

At any given temperature, the activity of SiO_2 at the electrode/hot metal interface is fixed by the auxiliary electrode, $ZrO_2 + ZrSiO_4$:

$$ZrO_2 + SiO_2 = ZrSiO_4 \qquad \ldots (50)$$

The oxygen potential at the three-phase interface of zirconia electrolyte + auxiliary electrode + liquid iron is established by the reaction

$$Si\,(\text{in iron}) + O_2(g) = SiO_2\,(\text{in zircon}) \qquad \ldots (51)$$

or alternatively by

$$ZrO_2(s) + Si\,(\text{in iron}) + O_2(g) = ZrSiO_4 \qquad \ldots (52)$$

Therefore,

$$\log K_{52} = -\log h_{Si} - \log P_{O_2} \qquad \ldots (53)$$

where K_{52} is the equilibrium constant for reaction (52) and h_{Si} is the Henrian activity of silicon in liquid iron. From Eq. (53) it is clear that h_{Si} correlates directly with P_{O_2}.

If *n*-type electronic conduction in the ZrO_2(MgO) used were negligible then the open circuit emf of the cell can be represented as

$$E - E_t = (RT/4F)\ln[P_{O_2}(\text{ref})/P_{O_2}(\text{test})]$$

$$= (RT/4F)\ln\{P_{O_2}(\text{ref})/[K_{52}h_{Si}]^{-1}\} \qquad \ldots (54)$$

where E is the cell emf and E_t is the thermal emf between Fe and Mo. If *n*-type conduction is not negligible open circuit emf is given by Eq. (41). The performance of the cell was tested in molten Fe + C + Si alloys at 1723 K. The measured cell potentials showed satisfactory sensitivity to the variation of silicon activity in the hot metal.

Non-isothermal Cells

Non-isothermal galvanic sensors are being introduced for continuous monitoring of the chemical potential of species in corrosive melts at high temperatures. The corrosive nature of the melt often destroys the ionic conducting properties of the solid electrolyte and thus degrades sensor response. A design solution to this problem consists in continuously introducing a new volume element of solid electrolyte into the melt at a rate commensurate with the rate of chemical reaction. Thus a functioning solid electrolyte is always in contact with the melt and the sensor can be used in a continuous mode. In this proposed 'feeder design' the end of the solid electrolyte rod away from the melt is at a lower temperature. The reference electrode is usually placed at the colder end (T_1). This minimizes the reaction between the reference electrode and the solid electrolyte. In this design the sensor is non-isothermal and the temperature of the reference electrode varies with time: the temperature increasing as the reference electrode moves towards the corrosive melt in the furnace at temperature (T_2). This difference in temperature between the two electrodes makes an additional contribution to the emf. Because of the larger distance between the sample electrode and the reference electrode and the lower temperature on the reference side, the resistence of the cell is much greater than in isothermal cells. Consequently oxygen semipermeability through the electrolyte is minimized. A theoretical equation for the emf of a non-isothermal cell has been derived recently from the phenomenological expressions of irreversible thermodynamics[51]. The results of the fundamental analysis can be visualised in terms of a simple additive model. The emf of a non-isothermal cell

$$T_1, P'_{O_2}|\text{CSZ}|P''_{O_2}, T_2 \qquad \ldots (\text{XVI})$$

can be written as the sum of two contributions, one for an isothermal cell with the same difference in oxygen partial pressures,

$$T_1, P'_{O_2}|\text{CSZ}|P''_{O_2}, T_1 \qquad \ldots (\text{XVII})$$

and the other for a thermocell with the same partial pressure of oxygen at both the electrodes but with a difference in temperature,

$$T_1, P''_{O_2}|\text{CSZ}|P''_{O_2}, T_2 \qquad \ldots (\text{XVIII})$$

The Seebeck coefficient (ε) of a thermocell incorporating an oxygen ion conducting solid electrolyte is given by[51]

$$\varepsilon = dE/dT = \{2\tilde{S}(O^{2-}) - 4\tilde{S}(e, Pt) - S(O_2)\}/(4F) \qquad \ldots (55)$$

where $\tilde{S}(O^{2-})$ and $\tilde{S}(e, Pt)$ are the entropies of transport of O^{2-} ions in the solid electrolytes and electrons in platinum and $S(O_2)$ is the partial molar entropy of oxygen in the atmosphere at the electrodes. In pure oxygen $S(O_2)$ is zero. Combining the two contributions, one obtains

$$E = \frac{RT_1}{4F}\ln\frac{P''_{O_2}}{P'_{O_2}} + \varepsilon_{O_2}(T_1 - T_2) \qquad \ldots (56)$$

where ε_{O_2} is the Seebeck coefficient in pure oxygen. In principle, Seebeck coefficient is only a function of composition and temperature of the solid electrolyte. However, careful and precise measurements show that the Seebeck coefficient is mildly sensitive to microstructure of the solid elec-

trolyte. The measurement of two temperatures in a non-isothermal cell is inconvenient. It is therefore useful to design temperature compensated reference electrodes for non-isothermal galvanic sensors. Theory and design of temperature compensated reference electrodes and experimental verification of the theory using fully stabilized ZrO_2(CaO) as the solid electrolytes are discussed by Jacob and Ramasesha[52]. The criterion for temperature conpensation for a non-isothermal cell using a solid oxygen ion conductor as the electrolyte is that the Seebeck coefficient of the non-isothermal cell should be equal to the relative partial molar entropy of oxygen in the reference electrode divided by $4F$ (ref. 52), i.e.

$$\varepsilon_{O_2} = (1/4F)\,\Delta S(O_2)$$

It has been found that Ni + NiO mixture provides approximate temperature compensation when used as a reference electrode. The emf of the thermocell with Ni + NiO at each electrode is close to zero. For exact temperature compensation NiO should be taken as a solid solution in MgO[52]. The principles of non-isothermal cells and temperature compensated reference electrodes outlined above are applicable to solid state cells incorporating a wide variety of solid electrolytes.

Errors and Calibration

Temperature gradient—If there is a temperature gradient across the solid electrolyte a part of the emf developed by the cell will be due to the thermoelectric effect. The magnitude of this varies with the partial entropy of oxygen at the electrodes.

Mass transport through the gas phase—If the two electrode compartments are not well separated the transport of the active species from the electrode with higher potential to the electrode with lower potential through the gas phase may occur giving rise to lower emf.

Permeability of the solid electrolyte—If the chemical potentials of the active species at the electrodes are significantly different, effects of the mass transfer through the solid electrolyte become important. The flux of the active species through the electrolyte will induce polarisation of the electrodes thereby lowering the sensor emf. This can be avoided by using reference electrodes having a chemical potential close to that of the working electrode. Point electrodes can be used to deflect the semipermeability flux from the measuring electrode.

Induced emf—The furnace windings can induce emf in the leads. This can be avoided by using a noninductively wound furnace or by shielding the cell with earthed metallic sheet. Filters for a.c. ripple across the cell leads can also be employed in industrial applications when errors of a few mV can be tolerated.

Tests for Correct Functioning

A number of tests can be performed to ensure that an isothermal solid state galvanic cell is functioning properly.

(1) The whole cell assembly should be gas tight. This can be ensured by evacuating it at high temperature and checking for any gas leakage between the electrode compartments or between the cell and the ambient atmosphere.

(2) The open circuit emf should be zero if the chemical potential of the active species is the same at the both electrodes. Non-zero values with identical electrodes usually suggests the presence of thermal gradients across the cell.

(3) For a fixed gas composition at the electrodes, the emf plotted as a function of absolute temperature should be a straight line with a slope equal to the theoretical value defined by the Nernst equation. The line should pass through the origin.

(4) Cell reversibility can be checked by coulometric titration. The sensor emf should return to its original value before titration after a small quantity of current is passed through the sensor in either direction.

(5) The emf should be reproducible on temperature cycling.

(6) The small variations in the flow rate of the gases through the cell should not affect the emf. Flow rate dependence is indicative of gas phase polarisation or interference by residual oxygen in the inert gas.

(7) Keeping the reference gas composition at a constant value the test gas composition is altered by a known amount using an electrochemical pump. The resulting gas composition determined by a sensor should match the new value calculated from the pumping current.

Directions for Future Development

Future research is likely to concentrate on three principal aspects: (1) lower cost devices, (2) miniaturization, and (3) lower temperature of operation.

In order to achieve these, improvements in the solid electrolytes, electrodes and cell designs are essential. At low temperatures the electrode/electrolyte interfacial impedance makes a significant contribution to the total cell resistance[53]. It has

been found that the total resistance of an oxygen sensor based on zirconia electrolyte can be lowered using urania-50% scandia as the electrode material instead of platinum[54]. A combination of the above electrode with 30% platinum is found to be a better choice bringing down the operating temperature to 598 K[55]. A film of RuO_2 when used as an electrode for low temperature measurements in oxygen sensors based on zirconia electrolyte has been found to give theoretical emf down to 498 K compared to 923 K with platinum electrodes[56]. The decomposition of RuO_2 sets the low oxygen potential limit for the use of this electrode.

In most of the practical cases sensors are operated above 773 K. There are a number of advantages in finding materials that give reliable results at lower temperatures. The major advantages are low power requirement to maintain the device at its operating temperature and greater portability because a low power requirement can be satisfied with an electrochemical power source. In some applications involving hot gases the device might not require an additional heat source. A limiting factor in reducing the operating temperature is the increased cell resistance at low temperatures. Solid electrolyes having higher ionic conductivity such as $PbSnF_4$[57] have been developed for the measurement of oxygen partial pressure in the temperature range 423-473 K. The response time of the cell

$$Pt, Sn + SnF_2 | PbSnF_4 | RuO_2(powder), O_2, Pt \quad \ldots (XIX)$$

is found to be of the order of 60 s in the temperature range 423-473 K for an oxygen partial pressure change from 10^2 to 10^5 Pa. It has been found that cells based on LaF_3 single crystal electrolyte

$$Sn, SnF_2 \left| \begin{matrix} LaF_3 \\ (Single\ crystal) \end{matrix} \right| O_2, Pt \quad \ldots (XX)$$

can respond to an oxygen partial change at 298 K in 120 s[58,59]. The proposed sensing mechanism[60] involves the reduction of oxygen molecule to peroxide ion at the sensing electrode:

$$O_2 + 2e = 2O^- \quad \ldots (57)$$

The O^- ions exchange with the lattice F^- ions of LaF_3 at the sensing electrode/electrolyte interface

$$O^- + F_{F^x} = O_{F^x} + F^- \quad \ldots (58)$$

The overall reaction at the sensing electrode can be described as

$$O_2 + 2e + 2F_{F^x} = 2O_{F^x} + 2F^- \quad \ldots (59)$$

where F_{F^x} and O_{F^x} stand for the F^- and O^- ions sitting at F^- sites of LaF_3, respectively. At the reference electrode the reaction

$$SnF_2 + 2e = Sn + 2F^- \quad \ldots (60)$$

takes place. The electrochemical equilibria at the two interfaces can be written as

$$\mu^S_{O_2} + 2\mu^S_{F_2} + 2\eta^S_e = 2\mu^S_{O_2} + 2\eta^S_{F^-} \quad \ldots (61)$$

$$\mu^R_{SnF_2} + 2\eta^R_e = \mu^R_{Sn} + 2\eta^R_{F^-} \quad \ldots (62)$$

where μ is the chemical potential, η is the electrochemical potential and the superscripts S and R represents the sensing electrode/electrolyte inferface and Sn/SnF_2 interface at the reference electrode, respectively. Since F^- ions are the mobile species, the equilbirium between the two interfaces can be represented as

$$\eta^S_{F^-} = \eta^R_{F^-} \quad \ldots (63)$$

and the sensor emf is given by

$$\eta^S_e - \eta^R_e = -FE \quad \ldots (64)$$

From Eqs (61)-(64) we get

$$E = \frac{(\mu^R_{Sn} - \mu^R_{SnF_2})}{2F} + \frac{\mu^S_{O_2}}{2F} + \frac{(\mu^S_{F_2} - \mu^S_{O_2})}{F} \quad \ldots (65)$$

$$E = \text{const} + \frac{RT}{nF} \ln(P_{O_2}) + \frac{(\mu^S_{F_2} - \mu^S_{O_2})}{F} \quad \ldots (66)$$

A plot of E against $\ln P_{O_2}$ will be linear if both μ_{F_2} and μ_{O_2} are constant at the interface (S). It has been found that oxygen sensor based on sputtered LaF_3 instead of LaF_3 single crystal has a faster response[60]. The LaF_3 film was deposited on a metallic tin plate by means of RF sputtering. SnF_2 layer at the interface between the Sn plate and LaF_3 film was produced by electrolysis at 1 μA for 5 min in air at room temperature. The use of the sputtered film of electrolyte will reduce the cost of fabrication and opens the way to miniaturisation and sensor integration.

Miniaturization of devices using microelectronic techniques are progressing. Thin deposited films of solid electrolytes have low resistance because of their small thickness. The heater can also be printed on to the substrate.

References

1 Ricket H, *Einfuhrung in die elektrochemie fester Stoffe*, (Springer, Berlin) 1973.
2 Weppner W, *Sensors and Actuators*, 12 (1987) 107.
3 Fouletier J, *Sensors and Actuators*, 3 (1982/83) 295.

4 Williams D E & McGeehin P, *Electrochemistry* (Royal Society of Chemistry, London) (1984) 246.
5 Fairbank L H, *Heat Treat Met*, 4 (1977) 95.
6 Young C T & Bode J D, *SAE Trans*, 88 (1979) 790143.
7 Agrawal Y K, Short D W, Gruenke R & Rapp R A, *J Electrochem, Soc*, 121 (1974) 354.
8 Faultier J, Vitter G & Kleitz M, *J Appl Electrochem*, 5 (1975) 111.
9 Hamann E, Manger H & Steinke L, *Tech Paper SAE*, 7 (1977) 770401.
10 Eddy D S, *IEEE Trans Veh Technol*, VT23 (1974) 125.
11 Butler E P, Slotwinski R K, Bonanos N, Drennan J & Steele B C H, in '*Science and technology of zirconia II*', *Advances in ceramics*, Vol 12, edited by N, Claussen, M Ruhle and A H Heuer (American Ceramic Society, Columbs, Ohio, USA) 1984, 572.
12 Bonanos N, Slotwinski R K, Steele B C H & Butler E P, *J Mater Sci Lett*, 3 (1984) 245.
13 Wang D Y & Nowick A S, *J Electrochem Soc*, 126 (1977) 1155.
14 Verkerk M J, Hammink M W J & Burggraaf A J, *J Electrochem Soc*, 130 (1983) 70.
15 Schouler E J L, *Solid State Ionics*, 9/10 (1983) 945.
16 Alcock C B & Zador S, *J Appl Electrochem*, 2 (1972) 289.
17 Krafthefer B, Bohrer P, Moenkhaus P, Zook D, Pertl L & Bonne U, in "*Science and technology of zirconia II*", *Advances in ceramics*, Vol 12, edited by N Claussen, M Ruhle and Heuer A H (American Ceramic Society, Coloumbs, Ohio, USA) 1984, 607.
18 Badwal S P S, de Bruin H J & Franklin A D, *Solid State Ionics*, 9/10 (1983) 973.
19 Halland D M, *J Electrochem Soc*, 127 (1980) 796.
20 Akila R, Jacob K T & Shukla A K, *Bull Mater Sci*, 8 (1986) 453.
21 Foultier J, Fabry P & Kleitz M, *J Electrochem Soc*, 123 (1976) 204.
22 Jacob K T, Iwase M & Waseda Y, *J Appl Electrochem*, 12 (1982) 55.
23 Beerkmas N M & Heijne L, *Electrochim Acta*, 21 (1976) 303.
24 Heyne L & den Engelsen D, *J Electrochem Soc*, 124 (1977) 727.
25 Maskell W C, *J Phys E: Sci Instrum*, 20 (1987) 1156.
26 Fouletier J, Seinera H & Kleitz M, *J Appl Electrochem*, 4 (1974) 305.
27 Anderson J E & Graves Y B, *J Appl Electrochem*, 12 (1982) 335.
28 Winnubst A J A, Scharnborg A H A, Burggraff A J, *J Appl Electrochem*, 15 (1985) 139.
29 Anderson J E & Graves Y B, *J Electrochem Soc*, 128 (1981) 294.
30 Langmuir T, *Trans Faraday Soc*, 17 (1922) 621.
31 Halland D M, *J Elecrochem Soc*, 127 (1980) 796.
32 Chase M W, Curnutt J L, Prophet H, McDonald R A & Syverud Y V, *J Phys Chem Ref Data*, 4 (1975) 1-175.
33 Schmalzried H, *Ber Bunsenges Phys Chem*, 66 (1962) 572.
34 Romero A R, Harkki J & Janke D, *Process Metall Steel Res*, 57 (1986) 636.
35 Iwase M & Mori T, *Can Metall Q*, 19 (1980) 285.
36 Wilder T C & Gälin W E, *Trans TMS AIME*, 245 (1969) 1287.
37 Lungsgaard J S, Malling J & Birchall M L S, *Solid State Ionics*, 7 (1982) 53.
38 Schoonman J, Franceschetti D R & Hanneken J W, *Ber Bunsenges Phys Chem*, 86 (1982) 701.
39 Lyon S B & Fray D J, *Solid State Ionics*, 9/10 (1983) 1295.
40 Kahil H, Forester M & Guitton J, in *Solid state protonic conductors for fuel cells and sensors*, Part III, edited by J B Goodenough, J Jenson & A Potier (Odense University Press, Odense) 1985, 84.
41 Kumar R V & Fray D J, *Sensors and Actuators*, 15 (1988) 185.
42 Jacob K T, Bhogeswara Rao D & Nelson H G, *J Electrochem Soc*, 125 (1978) 758.
43 Jacob K T, Iwase M & Waseda Y, *Adv Ceram Meter*, 4 (1986) 264.
44 Jacob K T & Waseda Y, Unpublished work.
45 Jacob K T, Iwase M & Waseda Y, *J Appl Electrochem*, 12 (1982) 55.
46 Jacob K T, Iwase M & Waseda Y, *Solid State Ionics*, 23 (1987) 245.
47 Akila R & Jacob K T, *Sensors and Actuators*, 16 (1989) 311.
48 Akila R & Jacob K T, *J Appl Electrochem*, 18 (1988) 245.
49 Maruyama T, Sasaki S & Saita Y, *Solid State Ionics*, 23 (1987) 113.
50 Iwase M, *Scand J Metall*, 17 (1988) 50.
51 Ramasesha S K & Jacob K T, *J Appl Electrochem*, 19 (1989) 394.
52 Jacob K T & Ramasesha S K, *Solid State Ionics*, 34 (1989) 161.
53 Badwal S P S, Banninster M J & Garret W C T, in '*Science and technology of zirconia II*', *Advances in ceramics*, Vol 12, edited by N Claussen, M Ruhle & A H Heuer (American Ceramic Society) 1984, 598.
54 Badwal S P S, *J Electroanal Chem*, 202 (1986) 93.
55 Badwal S P S, *J Electroanal Chem*, 161 (1984) 75.
56 Periaswamy G, Varamban S V, Babu S R & Mathews C K, *Solid State Ionics*, 26 (1988) 311.
57 Siebert E, Foultier J & Vilminot S, *Solid State Ionics*, 9/10 (1983) 1291.
58 Kuwata S, Miura N, Yamazoe N & Seiyama T, *Chem Lett*, (1984) 981.
59 Yamazoe N, Hisamoto J, Miura N & Kuwata S, *Senosrs and Actuators*, 12 (1987) 415.
60 Miura N, Hisamoto J & Yamazoe N, *Sensors and Actuators*, 16 (1989) 301.